# Consistent two-population lattice Boltzmann model for thermal flows

I. V. Karlin,* D. Sichau,† and S. S. Chikatamarla‡
*Aerothermochemistry and Combustion Systems Lab, ETH Zurich, 8092 Zurich, Switzerland*
(Received 28 June 2013; published 30 December 2013)

Theory of two-population lattice Boltzmann equations for thermal flow simulations is revisited. The present approach makes use of a consistent division of the conservation laws between the two lattices, where mass and the momentum are conserved quantities on the first lattice, and the energy is conserved quantity of the second lattice. The theory of such a division is developed, and the advantage of energy conservation in the model construction is demonstrated in detail. The present fully local lattice Boltzmann theory is specified on the standard lattices for the simulation of thermal flows. Extension to the subgrid entropic lattice Boltzmann formulation is also given. The theory is validated with a set of standard two-dimensional simulations including planar Couette flow and natural convection in two dimensions.

DOI: 10.1103/PhysRevE.88.063310 PACS number(s): 47.11.−j, 51.10.+y, 05.20.Dd

## I. INTRODUCTION

The lattice Boltzmann (LB) method is a remarkably successful kinetic-theory approach to computational fluid dynamics, with applications ranging from turbulence [1] to flows at a micron scale, porous media, and multiphase flows [2], to relativistic hydrodynamics and beyond [3]. The LB method solves numerically a fully discrete kinetic equation for populations $f_i(\boldsymbol{x},t)$, designed to reproduce the Navier-Stokes equations in the hydrodynamic limit. Populations correspond to discrete velocities $\boldsymbol{v}_i$ which fit into a regular spatial lattice with the nodes $\boldsymbol{x}$. This enables a simple and highly efficient "stream-along-links-and-equilibrate-at-nodes" realization of the LB algorithm.

The success of the LB method stays primarily with the incompressible flow simulation. In that case, the LB models on lattices with relatively few velocities are available and most commonly used [4–7]. Moreover, with the development of the unconditionally stable entropic lattice Boltzmann method (ELBM) [8], recently it became possible to address high Reynolds number flows in complex geometries [9,10].

However, a similarly robust extension of the LB models to thermal and compressible flows remains an open issue in spite of a number of suggestions. To that end, there are three possible approaches which have been explored in the literature. According to the first approach, lattices with more velocities are required in order to adequately represent the moment system necessary to recover the full thermal Navier-Stokes-Fourier equations. However, early attempts such as [11,12] were not successful as the correspondent LB models were found to be numerically unstable. With the recent progress of the theory of admissible higher-order lattices [13–17] a systematic development of thermal and compressible LB models has become possible. However, the use of higher-order lattices for these problems has been limited so far due to complexity of corresponding models. Clearly, more studies are still required along this line.

In the standard LB models, geometric constraints associated with the lattice is an obstacle to extending the method to fully compressible flows [18]. Recently, a thermal model with energy conservation was developed on the standard lattices [19]. This has been achieved at a price of introducing correction terms into the kinetic equation in order to circumvent the lack of isotropy. While viable, this numerical scheme still requires off-lattice evaluations.

Finally, a third type of model was considered in [20] based on two sets of populations for representing momentum and temperature dynamics on two coupled lattices. However, this coupling in the formulation of [20] is nonlocal which increases complexity of the LB model. In particular, such physical effects as viscous heating do not emerge naturally, and had to be introduced as forcing/source terms. As a result, the two-population model of [20] is rarely used beyond the natural convection setting where it is degraded to a simpler passive scalar advection-diffusion model [21]. Overall, the main issues with developing lattice Boltzmann models for thermal and compressible flows at present remain with their simplicity, robustness, stability, and the range of temperatures they can address.

In this paper, we revisit and extend the theory of two-population lattice Boltzmann models. Our motivation stems from an observation that the original consideration of [20] was based on a somewhat *ad hoc* choice of the conservation laws at the outset of building up the model. Specifically, it was the thermal energy which was taken as a local conservation for the second lattice. This deprives the model developed in [20] from simplicity and locality of the coupling between the two lattices. On the other hand, a more natural choice is the total energy as it is the physical quantity which is in fact conserved by the Boltzmann equation. As we shall demonstrate in this paper, the choice of the energy rather than the thermal energy has major implications to the lattice Boltzmann equation for thermal flows as it renders the local coupling of the two lattices. The advantage of the energy instead of the thermal energy for two-population lattice Boltzmann model construction has been already realized in the paper [22], and we shall discuss the difference of the present approach from that of [22] below.

Let us outline a systematic study. In Sec. II we shall develop the two-population lattice Boltzmann equation based on a

*karlin@lav.mavt.ethz.ch
†sichau@lav.mavt.ethz.ch
‡chikatamarla@lav.mavt.ethz.ch

 

consistent splitting of the conservation laws of mass, momentum, and energy. In Sec. II A, a general idea of splitting is presented, and it is specified for standard lattices in Sec. II B. In Sec. II C, we present in detail the derivation of the hydrodynamic equations for the present two-population model, and clearly demonstrate the difference from [20] brought about by the use of the physical conservation law of energy. In particular, we demonstrate that the fully local two-lattice Bhatnagar-Gross-Krook (BGK) model retains the feature of the fixed Prandtl number, familiar from the conventional kinetic theory. In Sec. II D, we extend the two-population BGK equation to a two-population kinetic model with a tailored Prandtl number while retaining locality. In Sec. II E, we give details of a simple realization of the present two-population models on standard lattices in two and three dimensions, while in Sec. II F the entropic lattice Boltzmann formulation is provided. We complete the theoretical consideration in Sec. II G with a detailed discussion of the differences of the present approach from Ref. [22]. The theory developed in Sec. II is validated numerically in Sec. III. The two-dimensional realization for both conventional and entropic LB formulations was tested with the planar Couette flow and the Rayleigh-Bénard natural convection problem. Finally, in Sec. IV we conclude with a discussion.

## II. TWO-POPULATION LATTICE BOLTZMANN EQUATIONS

### A. Splitting the conservation laws

Let us remember that the classical Boltzmann equation for a single-component fluid in $D$ dimensions has $D+2$ local conservation laws, corresponding to the number of particles (fluid density), $D$ components of the momentum, and the energy. Our objective is to split the $D+2$ conservation laws into two sets corresponding to the density and the momentum, and the energy conservation. The hydrodynamic fields (density $\rho$, momentum density $\rho u_\alpha$, $\alpha = 1,\ldots,D$, and energy density $\rho E$ are defined as follows:

$$\rho = \sum_{i=0}^{Q} f_i, \tag{1}$$

$$\rho u_\alpha = \sum_{i=0}^{Q} f_i v_{i\alpha}, \tag{2}$$

$$2\rho E = \sum_{i=0}^{Q} g_i. \tag{3}$$

Although, in principle, the number of velocities for representing the $f$ and $g$ kinetics need not be the same, we shall assume this without any restriction. The above definition allows one to introduce the temperature $T$,

$$D\rho T + \rho u^2 = 2\rho E. \tag{4}$$

In this section, we shall consider as a starting example the case of the single relaxation time Bhatnagar-Gross-Krook (BGK) kinetic equation,

$$f_i(\boldsymbol{x}+\boldsymbol{v}_i\delta t, t+\delta t) - f_i(\boldsymbol{x},t) = \omega\left(f_i^{\mathrm{eq}} - f_i\right), \tag{5}$$

$$g_i(\boldsymbol{x}+\boldsymbol{v}_i\delta t, t+\delta t) - g_i(\boldsymbol{x},t) = \omega\left(g_i^{\mathrm{eq}} - g_i\right). \tag{6}$$

In Eqs. (5) and (6), $\omega$ is the relaxation parameter related to the viscosity and the thermal conductivity (to be specified below), $\delta t$ is the time step, and $f_i^{\mathrm{eq}}$ and $g_i^{\mathrm{eq}}$ are local equilibria that satisfy the local conservation,

$$\rho = \sum_{i=0}^{Q} f_i^{\mathrm{eq}}, \tag{7}$$

$$\rho u_\alpha = \sum_{i=0}^{Q} f_i^{\mathrm{eq}} v_{i\alpha}, \tag{8}$$

$$2\rho E = \sum_{i=0}^{Q} g_i^{\mathrm{eq}}. \tag{9}$$

It should be stressed here (and will be demonstrated in detail in Sec. II C) that one *cannot* assume the relaxation parameter $\omega$ in the $g$-populations kinetics (6) different from that in the $f$-populations kinetic Eq. (5) since the BGK relaxation mechanism is assumed. This is a direct implication of our objective to splitting the null space of the collision operator, by choosing the conserved quantity—energy—as the local conservation for the $g$ dynamics. It hints at the essential difference of our approach from [20] where the thermal energy $E_{\mathrm{th}} = DT$ instead of the energy $E$ (4) was used as a fictitious local conservation law on the $g$ lattice.

Furthermore, the local equilibria on both the lattices need to satisfy a set of conditions for the higher-order (nonconserved) moments in order to recover the correct hydrodynamic limit. For $f_i^{\mathrm{eq}}$, these are

$$P_{\alpha\beta}^{\mathrm{eq}} = \sum_{i=0}^{Q} v_{i\alpha} v_{i\beta} f_i^{\mathrm{eq}} = \rho T \delta_{\alpha\beta} + \rho u_\alpha u_\beta, \tag{10}$$

$$\begin{aligned} Q_{\alpha\beta\gamma}^{\mathrm{eq}} &= \sum_{i=0}^{Q} v_{i\alpha} v_{i\beta} v_{i\gamma} f_i^{\mathrm{eq}} \\ &= \rho T(u_\alpha\delta_{\beta\gamma} + u_\beta\delta_{\alpha\gamma} + u_\gamma\delta_{\alpha\beta}) + \rho u_\alpha u_\beta u_\gamma. \end{aligned} \tag{11}$$

Moving onto the equilibrium for $g$ populations, we note that $g^{\mathrm{eq}}$ is required to reproduce pertinent moments of the equilibrium distribution of the energy, $G \sim |\boldsymbol{v}|^2 e^{-|\boldsymbol{v}-\boldsymbol{u}|^2/2T}$, rather than that of the velocity, $F \sim e^{-|\boldsymbol{v}-\boldsymbol{u}|^2/2T}$. The moments of the equilibrium energy distribution,

$$G_{lmn}^{\mathrm{eq}} = \rho(2\pi T)^{-D/2} \int v_x^l v_y^m v_z^n |\boldsymbol{v}|^2 e^{-\frac{|\boldsymbol{v}-\boldsymbol{u}|^2}{2T}} d^D\boldsymbol{v}, \tag{12}$$

can be compactly written as (for $D = 3$),

$$G_{lmn}^{\mathrm{eq}} = [O_x]^l [O_y]^m [O_z]^n (2\rho E), \tag{13}$$

where operators $O_\alpha$ acting on any function of the velocity $\boldsymbol{u}$ are defined as follows:

$$O_\alpha = T\frac{\partial}{\partial u_\alpha} + u_\alpha, \tag{14}$$

and where $2\rho E = D\rho T + \rho u^2$ is the energy density (4). In particular, the higher-order moments pertinent to the analysis

of the hydrodynamic limit are the equilibrium energy flux $q_\alpha^{\rm eq}$ and the once-contracted fourth-order moment $R_{\alpha\beta}^{\rm eq}$,

$$q_\alpha^{\rm eq} = \rho\left[T\frac{\partial}{\partial u_\alpha} + u_\alpha\right](DT + u^2), \tag{15}$$

$$R_{\alpha\beta}^{\rm eq} = \rho\left[T\frac{\partial}{\partial u_\alpha} + u_\alpha\right]\left[T\frac{\partial}{\partial u_\beta} + u_\beta\right](DT + u^2). \tag{16}$$

Identifying these with the pertinent higher-order moments of the equilibrium populations $g^{\rm eq}$, computing the derivatives in (15) and (16), and using once again the definition of the energy (4), we obtain

$$q_\alpha^{\rm eq} = \sum_{i=0}^{Q} g_i^{\rm eq} v_{i\alpha} = \rho u_\alpha((D+2)T + u^2), \tag{17}$$

$$\begin{aligned} R_{\alpha\beta}^{\rm eq} &= \sum_{i=0}^{Q} g_i^{\rm eq} v_{i\alpha} v_{i\beta} \\ &= \rho T((D+2)T + u^2)\delta_{\alpha\beta} + \rho u_\alpha u_\beta((D+4)T + u^2). \end{aligned} \tag{18}$$

In the next section we shall consider a specification of the above splitting of the conservation laws to the standard lattices.

### B. Standard lattices

In this paper we shall restrict our consideration to the well-studied so-called standard lattices, which are $D$-dimensional tensor products of the fundamental three-velocity set $V = \{-1,0,1\}$, with an optional pruning in three dimensions (these are the standard $D2Q9$, $D3Q27$, $D3Q19$, and $D3Q15$ lattices; see Sec. II E for details). The application of standard lattices reduces the conditions (10) and (11) to the following:

$$P_{\alpha\beta}^{\rm eq} = \sum_{i=0}^{Q} v_{i\alpha} v_{i\beta} f_i^{\rm eq} = \rho c_{\rm s}^2 \delta_{\alpha\beta} + \rho u_\alpha u_\beta, \tag{19}$$

$$Q_{\alpha\beta\gamma}^{\rm eq} = \sum_{i=0}^{Q} v_{i\alpha} v_{i\beta} v_{i\gamma} f_i^{\rm eq} = \rho c_{\rm s}^2 (u_\alpha \delta_{\beta\gamma} + u_\beta \delta_{\alpha\gamma} + u_\gamma \delta_{\alpha\beta}), \tag{20}$$

where

$$c_{\rm s}^2 = \tfrac{1}{3} \tag{21}$$

is the speed of sound in lattice units. It can be regarded as a reference temperature $T_0 = c_{\rm s}^2$ which we shall further use to save notation. The moments of the energy distribution function are then made consistent with the fixed reference temperature $T_0$ on the $f$ lattice by using the fixed-temperature operator $\tilde{O}_\alpha$,

$$\tilde{O}_\alpha = T_0\frac{\partial}{\partial u_\alpha} + u_\alpha, \tag{22}$$

instead of operators $O_\alpha$ (14) in (13). In particular, the higher-order moments pertinent to the analysis of the hydrodynamic limit (see Sec. II C) are the equilibrium energy flux $q_\alpha^{\rm eq}$ and the once-contracted fourth-order moment $R_{\alpha\beta}^{\rm eq}$,

$$q_\alpha^{\rm eq} = \sum_{i=0}^{Q} g_i^{\rm eq} v_{i\alpha} = \rho u_\alpha(DT + u^2) + 2\rho T_0 u_\alpha, \tag{23}$$

$$\begin{aligned} R_{\alpha\beta}^{\rm eq} &= \sum_{i=0}^{Q} g_i^{\rm eq} v_{i\alpha} v_{i\beta} \\ &= \rho(DT + u^2)(T_0\delta_{\alpha\beta} + u_\alpha u_\beta) + 2\rho T_0(T_0\delta_{\alpha\beta} + 2u_\alpha u_\beta). \end{aligned} \tag{24}$$

Note that the above conditions for the conserved and nonconserved moments do not uniquely specify the equilibrium populations. We shall postpone specification of the equilibria until Sec. II E. In the Sec. II C we shall derive the hydrodynamic limit of the BGK two-population system, assuming the above constraints are satisfied by the equilibria. Before we proceed, a few remarks are in order:

(1) The main limitation of the standard lattices is that they satisfy the constraint for the third-order moments at a fixed speed of sound $c_{\rm s}$ (20) rather than (11). This limitation is due to the lattice constraint, $v_{i\alpha}^3 = v_{i\alpha}$, which is pertinent to all standard lattices, and it restricts the use of the standard lattices to low Mach number flows. This is still a large class of flows for which efficient thermal flow LB model is needed.

(2) The consequence of the above restriction is that the adiabatic exponent of the model under consideration is $\gamma = 1$. Consequently, the Prandtl number, $\Pr = (\gamma\mu)/\kappa$ becomes $\Pr = \mu/\kappa$ where $\mu$ and $\kappa$ are kinematic viscosity and temperature conductivity, respectively.

### C. Hydrodynamic limit of the two-population BGK model

#### 1. Density and momentum equations

Here we derive the continuum limit of the kinetic equations (5) and (6). Let us begin with the $f$-populations dynamics (5) in order to establish the density and momentum equations. Since the standard constraints for the higher-order moments of $f$ populations, Eqs. (10) and (11), are assumed, this will result in the equation for the density and flow velocity as in the conventional LB model. We shall, however, display this derivation as parts of it will be used in the later analysis of the $g$ kinetics.

After expanding the shift operators into a Taylor series to second order,

$$\begin{aligned} &\left[\delta t(\partial_t + v_{i\mu}\partial_\mu) + \frac{\delta t^2}{2}(\partial_t + v_{i\mu}\partial_\mu)(\partial_t + v_{i\mu}\partial_\mu)\right] f_i \\ &\quad = \omega\left(f_i^{\rm eq} - f_i\right), \end{aligned} \tag{25}$$

let us introduce a characteristic time scale of the flow $\Theta$ and reduced time $t' = t/\Theta$. Furthermore, we introduce the reduced velocities $v_i' = v_i/c$, where $c = 1$, and reduced coordinate, $x' = x/(c\Theta)$. With this, (25) is rewritten in terms of derivatives with respect to primed variables, $t'$ and $x'$, and we omit primes in the sequel in order to simplify notation. Introducing a smallness parameter, $\epsilon = \delta t/\Theta$, and omitting terms of the

order $\epsilon^3$, Eq. (25) is written:

$$\left[\epsilon(\partial_t + v_{i\mu}\partial_\mu) + \frac{\epsilon^2}{2}(\partial_t + v_{i\mu}\partial_\mu)(\partial_t + v_{i\mu}\partial_\mu)\right] f_i = \omega\left(f_i^{\mathrm{eq}} - f_i\right). \tag{26}$$

Let us introduce a multiscale expansion of the time derivative to second order, and an expansion of the populations in terms of $\epsilon$ to second order,

$$\epsilon\partial_t = \epsilon\partial_t^{(1)} + \epsilon^2\partial_t^{(2)} + \ldots, \tag{27}$$

$$f_i = f_i^{(0)} + \epsilon f^{(1)} + \epsilon^2 f^{(2)} + \ldots. \tag{28}$$

Substituting (28) and (27) into (26), we analyze this equation to the order $\epsilon^2$. On order $\epsilon^0$, we find that the leading term in the expansion (28) is the local equilibrium,

$$f_i^{(0)} = f_i^{\mathrm{eq}}. \tag{29}$$

A further analysis makes use of the solvability condition: since local conservation laws imply

$$\sum_{i=0}^{Q}\{1, v_{i\alpha}\} f_i = \sum_{i=0}^{Q}\{1, v_{i\alpha}\} f_i^{\mathrm{eq}}, \tag{30}$$

from (28) it follows

$$\sum_{i=0}^{Q}\{1, v_{i\alpha}\} f_i^{(1)} = \sum_{i=0}^{Q}\{1, v_{i\alpha}\} f_i^{(2)} = \cdots = 0. \tag{31}$$

On the order $\epsilon^1$, we have

$$f_i^{(1)} = -\frac{1}{\omega}\left(\partial_t^{(1)} + v_{i\mu}\partial_\mu\right) f_i^{\mathrm{eq}}. \tag{32}$$

Applying solvability condition (31), we find the time derivatives of the hydrodynamic fields (density and momentum) at the first order:

$$\partial_t^{(1)}\rho = -\partial_\alpha(\rho u_\alpha), \tag{33}$$

$$\partial_t^{(1)} u_\alpha = -u_\beta\partial_\beta u_\alpha - \frac{1}{\rho}\partial_\alpha(\rho T_0). \tag{34}$$

Finally, on the order $\epsilon^2$, we have

$$\left[\partial_t^{(2)} - \left(\frac{1}{\omega} - \frac{1}{2}\right)\left(\partial_t^{(1)}\partial_t^{(1)} + v_{i\mu}v_{i\nu}\partial_\mu\partial_\nu + 2v_{i\mu}\partial_\mu\partial_t^{(1)}\right)\right] f_i^{(0)} = -\omega f_i^{(2)}. \tag{35}$$

Applying again solvability conditions (31), we find that the second-order contribution to the continuity equations vanishes:

$$\partial_t^{(2)}\rho = 0, \tag{36}$$

whereas the second-order term in the momentum equations is

$$\partial_t^{(2)}(\rho u_\alpha) = \left(\frac{1}{\omega} - \frac{1}{2}\right)\partial_\beta\left(\partial_t^{(1)} P_{\alpha\beta}^{\mathrm{eq}} + \partial_\gamma Q_{\alpha\beta\gamma}^{\mathrm{eq}}\right). \tag{37}$$

Note that, apart from the equilibrium pressure tensor already discussed above, the result (37) also depends on the equilibrium third-order moments of the $f$ populations. Computing the first-order time derivative of the function $P_{\alpha\beta}^{\mathrm{eq}}$ using chain rule and the result of the preceding order (33) and (34), for the density and velocity, and neglecting terms of the order of $O(u^3)$ as pertinent to the standard lattices we find

$$\partial_t^{(2)} u_\alpha = -\frac{1}{\rho}\partial_\beta\Pi_{\alpha\beta}, \tag{38}$$

where $\Pi_{\alpha\beta}$ is the nonequilibrium pressure tensor,

$$\Pi_{\alpha\beta} = -\mu\rho S_{\alpha\beta}, \tag{39}$$

and where we have introduced the rate-of-strain tensor $S_{\alpha\beta}$,

$$S_{\alpha\beta} = \partial_\alpha u_\beta + \partial_\beta u_\alpha, \tag{40}$$

and the kinematic viscosity $\mu$,

$$\mu = \left(\frac{1}{\omega} - \frac{1}{2}\right) T_0. \tag{41}$$

Summing up the contributions of the orders $\epsilon^1$ and $\epsilon^2$, we recover the continuity and the flow velocity equations,

$$\partial_t\rho = -\partial_\alpha(\rho u_\alpha), \tag{42}$$

$$\partial_t u_\alpha = -u_\beta\partial_\beta u_\alpha - \frac{1}{\rho}\partial_\alpha(\rho T_0) - \frac{1}{\rho}\partial_\beta\Pi_{\alpha\beta}. \tag{43}$$

### 2. *Temperature equation*

Similar analysis is now applied to the $g$-populations kinetic equation (6). For the sake of presentation, we start with a more general equation, introducing a different relaxation parameter $\omega_1$ into (6),

$$g_i(\boldsymbol{x} + \boldsymbol{v}_i\delta t, t + \delta t) - g_i(\boldsymbol{x}, t) = \omega_1\left(g_i^{\mathrm{eq}} - g_i\right). \tag{44}$$

The derivation below will demonstrate that the only consistent choice is $\omega_1 = \omega$.

Expanding (44) as above, introducing the expansion of the distribution function,

$$g_i = g_i^{(0)} + \epsilon g_i^{(1)} + \epsilon^2 g_i^{(2)} + \ldots, \tag{45}$$

and the multiscale expansion of the time derivative (27), we find on the order $\epsilon^0$:

$$g_i^{(0)} = g_i^{\mathrm{eq}}. \tag{46}$$

The counterpart of the solvability condition (31) is now based on the single conservation law of the $g$ kinetics:

$$\sum_{i=0}^{Q} g_i^{(1)} = \sum_{i=0}^{Q} g_i^{(2)} = \cdots = 0. \tag{47}$$

Using the latter on the orders $\epsilon^1$ and $\epsilon^2$, we find the pertinent time derivatives of the energy density $2\rho E = D\rho T + \rho u^2$ (4):

$$2\partial_t^{(1)}(\rho E) = -\partial_\alpha q_\alpha^{\mathrm{eq}}, \tag{48}$$

$$2\partial_t^{(2)}(\rho E) = \left(\frac{1}{\omega_1} - \frac{1}{2}\right)\partial_\alpha\left(\partial_t^{(1)} q_\alpha^{\mathrm{eq}} + \partial_\beta R_{\alpha\beta}^{\mathrm{eq}}\right). \tag{49}$$

Using the explicit form of the equilibrium energy flux $q_\alpha^{\mathrm{eq}}$ (23), and the first-order time derivatives of the density and of the velocity derived above [see Eqs. (33) and (34)], in (48), we obtain the first-order derivative of the temperature:

$$\partial_t^{(1)} T = -u_\alpha\partial_\alpha T - \frac{2}{D}T_0(\partial_\alpha u_\alpha). \tag{50}$$

This recovers the nondissipative part of the temperature equation of ideal fluid, with the restricted form of the compression work contribution, $-(2/D)T_0(\partial_\alpha u_\alpha)$ instead of $-(2/D)T(\partial_\alpha u_\alpha)$. This is consistent with the use of standard lattices as they are pertinent to the quasiincompressible flow simulation, in which the compression work is negligible.

Let us switch to the analysis of the second-order contribution to the temperature equation on the basis of (49). The left-hand side of (49) is transformed using the above results for the second-order time derivatives of the density (36) and of the flow velocity (38),

$$\partial_t^{(2)}(D\rho T + \rho u^2) = D\rho\partial_t^{(2)}T - 2u_\alpha\partial_\beta\Pi_{\alpha\beta}, \tag{51}$$

where the nonequilibrium pressure tensor $\Pi_{\alpha\beta}$ is given by Eq. (39). Let us transform the expression in the right-hand side of (49) using the explicit form of the functions $q_\alpha^{\rm eq}$ (23) and $R_{\alpha\beta}^{\rm eq}$ (24), and the first-order time derivatives of the hydrodynamic fields already obtained; we find after some algebra:

$$\partial_t^{(1)}q_\alpha^{\rm eq} + \partial_\beta R_{\alpha\beta}^{\rm eq} = D\rho T_0\partial_\alpha T + 2\rho T_0 u_\beta S_{\alpha\beta}. \tag{52}$$

Substituting (52) into the right-hand side of (49), and equating the result with (51), we find, using the explicit form of the nonequilibrium pressure tensor (39),

$$\partial_t^{(2)}T = \frac{2}{D\rho}(\partial_\alpha u_\beta)\left[\left(\frac{1}{\omega_1}-\frac{1}{2}\right)\rho T_0 S_{\alpha\beta}\right] + \frac{2}{D\rho}\left(\frac{1}{\omega_1}-\frac{1}{\omega}\right) \times u_\beta\partial_\alpha(\rho T_0 S_{\alpha\beta}) + \frac{1}{\rho}\left(\frac{1}{\omega_1}-\frac{1}{2}\right)\partial_\alpha\left[\rho T_0\partial_\alpha T\right]. \tag{53}$$

The choice of the relaxation parameter $\omega_1$ is dictated by two conditions:

(1) The first term in the right-hand side of (53) should give the viscous heating contribution consistent with the nonequilibrium pressure tensor $\Pi_{\alpha\beta}$ (39):

$$\frac{1}{\omega_1}-\frac{1}{2} = \frac{1}{\omega}-\frac{1}{2}. \tag{54}$$

(2) The anomalous second term in the right-hand side of (53) should vanish:

$$\frac{1}{\omega_1}-\frac{1}{\omega} = 0. \tag{55}$$

These two conditions are degenerate, and are satisfied simultaneously if and only if the relaxation parameters in the BGK equations for $f$ and $g$ populations are equal:

$$\omega_1 = \omega. \tag{56}$$

With (56) the remaining terms give the second-order time derivative of the temperature in the following form:

$$\partial_t^{(2)}T = \frac{1}{\rho}\partial_\alpha\left[\left(\frac{1}{\omega}-\frac{1}{2}\right)\rho T_0\partial_\alpha T\right] - \frac{2}{D\rho}(\partial_\alpha u_\beta)\Pi_{\alpha\beta}. \tag{57}$$

Summing up the first-order and second-order contributions to the temperature equation, we find

$$\partial_t T = -u_\alpha\partial_\alpha T - \frac{2}{D}T_0\partial_\alpha u_\alpha - \frac{2}{D\rho}(\partial_\alpha u_\beta)\Pi_{\alpha\beta} + \frac{1}{\rho}\partial_\alpha(\kappa\rho\partial_\alpha T). \tag{58}$$

Thus, the temperature equation of a quasi-incompressible fluid is recovered: The first term in the right-hand side is the advection of the temperature field by the velocity field, the second term is the (negligible) compression work, the third term corresponds to the viscous heating [$\Pi_{\alpha\beta}$ is the nonequilibrium pressure tensor (39)], while the last term is the Fourier law of heat dissipation, with the thermal conductivity coefficient $\kappa$,

$$\kappa = \left(\frac{1}{\omega}-\frac{1}{2}\right)T_0. \tag{59}$$

Before proceeding further, a few comments about the present derivation are in order:

(1) The coupling between the $f$ and $g$ lattices is local, as pertinent for the efficient LB model. This roots in the fact that we used the energy $2\rho E = D\rho T + \rho u^2$ as the primary (locally conserved) field rather than the thermal energy $2\rho E_{\rm th} = D\rho T$ as in the previous two-population model [20].

(2) With the specified restrictions from the use of the standard lattices, the present model recovers in a natural and straightforward way the temperature equation. It should be noted specifically that the viscous dissipation arises in a natural way in the present approach unlike in the previous model [20] where it had to be put in by an additional forcing term in the $g$-population equation. This proves that the present model is the natural candidate to replace the model of [20] for the similar flow problems.

(3) The simple LBGK collision integral used above does not allow one to choose independently the relaxation parameters in the $f$- and $g$-populations dynamics. This is expected since the recovery of the correct temperature equation requires that the two dissipation processes (heat dissipation and viscous heating) to be matched in the second-order time derivative of the temperature where the viscosity coefficient has been already specified. This forces the Prandtl number of the present model, $\Pr = (\gamma\mu)/\kappa$ ($\gamma = 1$) to be fixed at $\Pr = 1$.

In the next section we shall correct the latter problem by considering a more general but still locally coupled LB model.

### D. Variable Prandtl number

Let us remember that in order to derive a lattice Boltzmann model with a given Prandtl number, one needs to introduce intermediate (quasiequilibrium) states of relaxation, in addition to the equilibrium. In the single-lattice setting, the corresponding quasiequilibrium model has been described in [23], based on the kinetic theory paradigm [24,25]. In the present two-population setting, the quasiequilibrium model with the tailored Prandtl number is proposed in the following form:

$$f_i(\boldsymbol{x}+\boldsymbol{v}_i\delta t, t+\delta t) - f_i(\boldsymbol{x},t) = \omega\left(f_i^{\rm eq} - f_i\right), \tag{60}$$

$$g_i(\boldsymbol{x}+\boldsymbol{v}_i\delta t, t+\delta t) - g_i(\boldsymbol{x},t) = \omega_1(g_i^* - g_i) + \omega_2\left(g^{\rm eq} - g_i^*\right), \tag{61}$$

where the equilibria for both the lattices are as above, while the quasiequilibrium $g_i^*$ satisfies the conservation of energy (3) and the equilibrium constraint (24),

$$\sum_{i=0}^{Q} g_i^* = 2\rho E, \tag{62}$$

$$\sum_{i=0}^{Q} g_i^* v_{i\alpha} v_{i\beta} = R_{\alpha\beta}^{\mathrm{eq}}, \tag{63}$$

along with the following condition for the (nonequilibrium) energy flux:

$$\sum_{i=0}^{Q} g_i^* v_{i\alpha} = q_\alpha^{\mathrm{eq}} + 2u_\beta\left(P_{\alpha\beta} - P_{\alpha\beta}^{\mathrm{eq}}\right). \tag{64}$$

In other words, the quasiequilibrium $g^*$ differs from the equilibrium $g^{\mathrm{eq}}$ by the nonequilibrium energy flux (64) only. The condition (64) describes the quasiequilibrium in which the equilibrium energy flux is extended by a nonequilibrium component due to the nonequilibrium pressure tensor evaluated on $f$ populations,

$$P_{\alpha\beta} = \sum_{i=0}^{Q} f_i v_{i\alpha} v_{i\beta}.$$

Kinetic equations (60) and (61) and next analyzed as above. To that end, we note that the zeroth-order solution remains as before, $f_i^{(0)} = f_i^{\mathrm{eq}}$, $g_i^{(0)} = g_i^{\mathrm{eq}}$; thus, the first-order time derivatives of the density and velocity are given by Eqs. (33) and (34). Furthermore, from the first-order equation of the $g$-population kinetics,

$$g_i^{(1)} = -\frac{1}{\omega_1}\left(\partial_t^{(1)} + v_{i\alpha}\partial_\alpha\right) g_i^{\mathrm{eq}} + \left(1 - \frac{\omega_2}{\omega_1}\right) g_i^{*(1)}, \tag{65}$$

we immediately conclude that also the first-order time derivative of the temperature is given by Eq. (50). Consequently, up to second order, the continuity and the velocity equations are recovered in the above form, Eqs. (42) and (43). Finally, the second-order time derivative of the energy becomes

$$\begin{aligned} 2\partial_t^{(2)}(\rho E) = {} & \left(\frac{1}{\omega_1} - \frac{1}{2}\right)\partial_\alpha\left(\partial_t^{(1)} q_\alpha^{\mathrm{eq}} + \partial_\beta R_{\alpha\beta}^{\mathrm{eq}}\right) \\ & - \left(1 - \frac{\omega_2}{\omega_1}\right)\partial_\alpha q_\alpha^{*(1)}, \end{aligned} \tag{66}$$

where the right-hand side differs from (49) by the divergence of the the quasiequilibrium energy flux $q_\alpha^{*(1)} = \sum_{i=0}^{Q} g_i^{*(1)} v_{i\alpha}$. For the quasiequilibrium model with the constraint (64), the quasiequilibrium energy flux is given by the nonequilibrium part of the pressure tensor,

$$q_\alpha^{*(1)} = 2u_\beta P_{\alpha\beta}^{(1)} = 2u_\beta \sum_{i=1}^{Q} f_i^{(1)} v_{i\alpha} v_{i\beta} = -2\left(\frac{1}{\omega}\right)\rho T_0 u_\beta S_{\alpha\beta}. \tag{67}$$

With (67), and using the above results (51) and (52), we find the second-order time derivative of the temperature,

$$\begin{aligned} \partial_t^{(2)} T = {} & \frac{2}{D\rho}\left\{\left(\frac{1}{\omega_1} - \frac{1}{2}\right) + \frac{1}{\omega}\left(1 - \frac{\omega_2}{\omega_1}\right)\right\}(\partial_\alpha u_\beta)(\rho T_0 S_{\alpha\beta}) \\ & + \frac{2}{D\rho}\left\{\left(\frac{1}{\omega_1} - \frac{1}{\omega}\right) + \frac{1}{\omega}\left(1 - \frac{\omega_2}{\omega_1}\right)\right\} u_\beta \partial_\alpha(\rho T_0 S_{\alpha\beta}) \\ & + \frac{1}{\rho}\left(\frac{1}{\omega_1} - \frac{1}{2}\right)\partial_\alpha\left(\rho T_0 \partial_\alpha T\right). \end{aligned} \tag{68}$$

Similar to the case of BGK (53), the choice of $\omega_2$ is due to two conditions: The first term on the right-hand side of (68) should give a consistent viscous dissipation contribution,

$$\left(\frac{1}{\omega_1} - \frac{1}{2}\right) + \frac{1}{\omega}\left(1 - \frac{\omega_2}{\omega_1}\right) = \frac{1}{\omega} - \frac{1}{2}. \tag{69}$$

At the same time, the second (anomalous) term on the right-hand side of (68) should vanish,

$$\left(\frac{1}{\omega_1} - \frac{1}{\omega}\right) + \frac{1}{\omega}\left(1 - \frac{\omega_2}{\omega_1}\right) = 0. \tag{70}$$

Both (69) and (70) are satisfied simultaneously by the following choice of $\omega_2$:

$$\omega_2 = \omega. \tag{71}$$

Thus, the temperature equation is recovered in the form of (58) where the thermal conductivity $\kappa$ is now ruled by the relaxation parameter $\omega_1$, independent of the viscosity relaxation parameter $\omega$,

$$\kappa = \left(\frac{1}{\omega_1} - \frac{1}{2}\right) T_0, \tag{72}$$

so that the Prandtl number is

$$\mathrm{Pr} = \frac{\mu}{\kappa} = \frac{2-\omega}{2-\omega_1}. \tag{73}$$

We shall now proceed with finalizing the construction of the consistent two-population LB equation for thermal flows by specifying the equilibria and quasiequilibria.

### E. Realization of the consistent thermal lattice Boltzmann model on standard lattices

In summary, the two-population lattice Boltzmann equation developed above is written in the standard form in lattice units ($\delta t = 1$):

$$f_i(\boldsymbol{x} + \boldsymbol{v}_i, t+1) - f_i(\boldsymbol{x}, t) = \omega\left(f_i^{\mathrm{eq}} - f_i\right), \tag{74}$$

$$g_i(\boldsymbol{x} + \boldsymbol{v}_i, t+1) - g_i(\boldsymbol{x}, t) = \omega_1(g_i^* - g_i) + \omega\left(g_i^{\mathrm{eq}} - g_i^*\right). \tag{75}$$

The equilibrium populations $f_i^{\mathrm{eq}}$ and $g_i^{\mathrm{eq}}$, and the quasiequilibrium population $g_i^*$ are constructed from a single form (sometimes called Grad distribution [26]),

$$\begin{aligned} F_i = W_i \Bigg( & M_0 + \frac{M_\alpha v_{i\alpha}}{T_0} \\ & + \frac{(M_{\alpha\beta} - M_0 T_0 \delta_{\alpha\beta})(v_{i\alpha} v_{i\beta} - T_0 \delta_{\alpha\beta})}{2T_0^2} \Bigg). \end{aligned} \tag{76}$$

TABLE I. Corresponding weights for each contributing shell.

| $V_i$ | $D3Q27$ | $D3Q19$ | $D3Q15$ |
|---|---|---|---|
| $V_0$ | 8/27 | 1/3 | 2/9 |
| $V_1$ | 2/27 | 1/18 | 1/9 |
| $V_2$ | 1/54 | 1/36 | 0 |
| $V_3$ | 1/216 | 0 | 1/72 |

For the planar $D2Q9$ lattice, composed of the energy shells $V_0 = \{(0,0)\}$, $V_1 = \{(\pm1,0),(0,\pm1)\}$, and $V_2 = \{(\pm1,\pm1)\}$, the weights $W_i$ are equal for all the velocities in each shell, $W_0 = 4/9$, $W_1 = 1/9$, and $W_2 = 1/36$ for $V_0$, $V_1$, and $V_2$, respectively. For the standard lattices in three dimensions, the velocity vectors are represented as three combinations of the energy shells $V_i$, $i = 0,1,2,3$ where

$$
\begin{aligned}
V_0 &= \{(0,0,0)\},\\
V_1 &= \{(\pm1,0,0),(0,\pm1,0),(0,0,\pm1)\},\\
V_2 &= \{(\pm1,\pm1,0),(\pm1,0,\pm1),(0,\pm1,\pm1)\},\\
V_3 &= \{(\pm1,\pm1,\pm1)\}.
\end{aligned}
$$

Using the standard nomenclature, these lattices are

$$
\begin{aligned}
D3Q27 &= V_0 \cup V_1 \cup V_2 \cup V_3,\\
D3Q19 &= V_0 \cup V_1 \cup V_2,\\
D3Q15 &= V_0 \cup V_1 \cup V_3,
\end{aligned}
$$

while the corresponding weights $W_i$ for each contributing shell are shown in Table I.

Finally, $T_0 = 1/3$ for all the lattices mentioned. Relevant equilibria and quasiequilibria are obtained upon the following (Table II) substitutions in place of $M_0$, $M_\alpha$, and $M_{\alpha\beta}$ in the generic form (76), where the primary (locally conserved) fields $\rho$, $\rho u_\alpha$, and $2\rho E$ are

TABLE II. Substitutions for $M_0, M_\alpha$, and $M_{\alpha\beta}$.

| | $M_0$ | $M_\alpha$ | $M_{\alpha\beta}$ |
|---|---|---|---|
| $f_i^{\mathrm{eq}}$ | $\rho$ | $\rho u_\alpha$ | $P_{\alpha\beta}^{\mathrm{eq}}$ |
| $g_i^{\mathrm{eq}}$ | $2\rho E$ | $q_\alpha^{\mathrm{eq}}$ | $R_{\alpha\beta}^{\mathrm{eq}}$ |
| $g_i^{*}$ | $2\rho E$ | $q_\alpha^{\mathrm{eq}} + 2u_\beta\left(P_{\alpha\beta} - P_{\alpha\beta}^{\mathrm{eq}}\right)$ | $R_{\alpha\beta}^{\mathrm{eq}}$ |

$$\rho = \sum_{i=0}^{Q} f_i, \tag{77}$$

$$\rho u_\alpha = \sum_{i=0}^{Q} f_i v_{i\alpha}, \tag{78}$$

$$2\rho E = \sum_{i=0}^{Q} g_i, \tag{79}$$

and the higher-order moments are

$$P_{\alpha\beta}^{\mathrm{eq}} = \rho T_0 \delta_{\alpha\beta} + \rho u_\alpha u_\beta, \tag{80}$$

$$P_{\alpha\beta} = \sum_{i=0}^{Q} f_i v_{i\alpha} v_{i\beta}, \tag{81}$$

$$q_\alpha^{\mathrm{eq}} = 2\rho E u_\alpha + 2\rho T_0 u_\alpha, \tag{82}$$

$$R_{\alpha\beta}^{\mathrm{eq}} = 2\rho E(T_0\delta_{\alpha\beta} + u_\alpha u_\beta) + 2\rho T_0(T_0\delta_{\alpha\beta} + 2u_\alpha u_\beta). \tag{83}$$

Explicitly, the equilibria $f_i^{\mathrm{eq}}$, $g_i^{\mathrm{eq}}$ and the quasiequilibrium $g_i^{*}$ are

$$f_i^{\mathrm{eq}} = W_i\left(\rho + \frac{\rho u_\alpha v_{i\alpha}}{T_0} + \frac{\left(P_{\alpha\beta}^{\mathrm{eq}} - \rho T_0\delta_{\alpha\beta}\right)\left(v_{i\alpha}v_{i\beta} - T_0\delta_{\alpha\beta}\right)}{2T_0^2}\right); \tag{84}$$

$$g_i^{\mathrm{eq}} = W_i\left(2\rho E + \frac{q_\alpha^{\mathrm{eq}} v_{i\alpha}}{T_0} + \frac{\left(R_{\alpha\beta}^{\mathrm{eq}} - 2\rho E T_0\delta_{\alpha\beta}\right)\left(v_{i\alpha}v_{i\beta} - T_0\delta_{\alpha\beta}\right)}{2T_0^2}\right); \tag{85}$$

$$g_i^{*} = W_i\left(2\rho E + \frac{\left(q_\alpha^{\mathrm{eq}} + 2u_\beta\left(P_{\alpha\beta} - P_{\alpha\beta}^{\mathrm{eq}}\right)\right)v_{i\alpha}}{T_0} + \frac{\left(R_{\alpha\beta}^{\mathrm{eq}} - 2\rho E T_0\delta_{\alpha\beta}\right)\left(v_{i\alpha}v_{i\beta} - T_0\delta_{\alpha\beta}\right)}{2T_0^2}\right). \tag{86}$$

Note that the equilibrium for the $f$ populations $f_i^{\mathrm{eq}}$ (84) is the standard quadratic equilibrium of the conventional LB model [6].

The temperature is computed according to the energy definition (4):

$$T = \frac{\sum_{i=0}^{Q} g_i - \left(\sum_{i=0}^{Q} f_i v_{i\alpha}\right)\left(\sum_{i=0}^{Q} f_i v_{i\alpha}\right)\left(\sum_{i=0}^{Q} f_i\right)^{-1}}{D\sum_{i=0}^{Q} f_i}. \tag{87}$$

The present two-population lattice Boltzmann equation recovers hydrodynamic equations in the following form:

$$\partial_t \rho = -\partial_\alpha(\rho u_\alpha), \tag{88}$$

$$\partial_t u_\alpha = -u_\beta\partial_\beta u_\alpha - \frac{1}{\rho}\partial_\alpha\left(\rho c_{\mathrm{s}}^2\right) - \frac{1}{\rho}\partial_\beta\Pi_{\alpha\beta}, \tag{89}$$

$$\partial_t T = -u_\alpha \partial_\alpha T - \frac{2}{D} c_s^2 \partial_\alpha u_\alpha - \frac{2}{D\rho}(\partial_\alpha u_\beta)\Pi_{\alpha\beta} + \frac{1}{\rho}\partial_\alpha (\kappa \rho \partial_\alpha T), \quad (90)$$

where the viscous pressure tensor $\Pi_{\alpha\beta}$ is

$$\Pi_{\alpha\beta} = -\mu\rho(\partial_\alpha u_\beta + \partial_\beta u_\alpha), \quad (91)$$

and the kinematic viscosity $\mu$ is

$$\mu = \left(\frac{1}{\omega} - \frac{1}{2}\right) c_s^2, \quad (92)$$

and the thermal conductivity $\kappa$ is

$$\kappa = \left(\frac{1}{\omega_1} - \frac{1}{2}\right) c_s^2, \quad (93)$$

while $c_s^2 = T_0 = 1/3$. We shall make a few comments at this point.

(1) Unlike the original two-population LB model [20], the present LB equation is completely local and is easy to implement in the same way as the standard LB equation;

(2) For the standard lattices considered above, the present local LB equation nevertheless recovers the same hydrodynamics as the model [20]. In particular, the viscous heating and adjustable Prandtl number appear naturally from the local coupling between the two lattices (via corresponding equilibria and quasiequilibria), and there is no need to reintroduce these effects by a force or source term like in the models considered in [20] or [19].

(3) Consequently, there is no need for a simplification in the manner of [21] which neglects the "inconvenient" terms in the model of [20]. From the present theory standpoint, this would correspond to the following constraints for $q_\alpha^{\rm eq}$ and $R_{\alpha\beta}^{\rm eq}$ instead of (23) and (24), respectively,

$$q_\alpha^{\rm eq} = \sum_{i=0}^{Q} g_i^{\rm eq} v_{i\alpha} = \rho u_\alpha (DT + u^2), \quad (94)$$

$$R_{\alpha\beta}^{\rm eq} = \sum_{i=0}^{Q} g_i^{\rm eq} v_{i\alpha} v_{i\beta} = \rho(DT + u^2)(T_0\delta_{\alpha\beta} + u_\alpha u_\beta), \quad (95)$$

or, in other words, $q_\alpha^{\rm eq}$ and $R_{\alpha\beta}^{\rm eq}$ are assumed to be proportional to the flow velocity and the equilibrium pressure tensor, $q_\alpha^{\rm eq} = 2\rho E u_\alpha$, and $R_{\alpha\beta}^{\rm eq} = 2E P_{\alpha\beta}^{\rm eq}$. As a consequence, instead of (85), we would simply get $g_i^{\rm eq} = 2E f_i^{\rm eq}$, while only the advection and the thermal conductivity terms in the temperature equation will be recovered. It can be argued that such a simplification can still be useful for a number of flows where viscous heating due to shear is not significant. However, such a simplification clearly contradicts the kinetic theory constraints and is merely a convenience assumption based on the need to simplify the model [20]. In the present approach, as the local coupling between the two lattices is robust and delivers the full thermal equation (with a restriction only due to the choice of the standard lattices), such a simplification is neither needed nor required.

### F. Entropic lattice Boltzmann realization

Finally, the above two-population LB equation can be enhanced to the entropic lattice Boltzmann method (ELBM) [8] if subgrid simulations are of concern. To that end, the entropy function for the $f$ populations is defined in the usual way [8]:

$$H(f) = \sum_{i=0}^{Q} f_i \ln\left(\frac{f_i}{W_i}\right), \quad (96)$$

where the weights are the same as above in II E. Instead of the system (74) and (75), we have

$$f_i(\boldsymbol{x} + \boldsymbol{v}_i, t+1) - f_i(\boldsymbol{x}, t) = \alpha\beta\left(f_i^{\rm eq} - f_i\right), \quad (97)$$

$$g_i(\boldsymbol{x} + \boldsymbol{v}_i, t+1) - g_i(\boldsymbol{x}, t) = \omega_1(g_i^* - g_i) + 2\beta\left(g_i^{\rm eq} - g_i^*\right). \quad (98)$$

Here the same equilibria and quasiequilibria as above are used, while the fixed relaxation parameter $\omega$ in the $f$ equation is replaced by $\alpha\beta$ where $\alpha$ is the maximal overrelaxation, which is operationally available as the positive root of the entropy condition:

$$H(f + \alpha(f^{\rm eq} - f)) = H(f). \quad (99)$$

The viscosity is parametrized with $\beta \in [0,1]$ instead of $\omega = 2\beta$, so that

$$\mu = \frac{1}{2}\left(\frac{1}{\beta} - 1\right) c_s^2. \quad (100)$$

The equilibrium (84) used in the ELBM equation (97) and in the entropy estimate (99) is the approximation to the minimizer of the entropy function (96) to the overall accuracy of the LB method in terms of the flow velocity (cf., e.g., [8,9]).

In other words, the entropic lattice Boltzmann stabilization procedure is applied only on the $f$-populations kinetic equation (97) while the $g$-populations equation (98) remains the same as in the standard LB realization, Eq. (75), with an appropriate re-parametrization. This is consistent in the present context which uses the standard lattices since the system (74) and (75) [or (97) and (98)] is coupled in one way only; that is, the information gathered from the $f$ lattice (density and velocity) is provided to the equilibrium and the quasiequilibrium of the $g$ lattice. Consequently, application of ELBM in the present context is to capture the subgrid dynamics of the velocity only. We shall proceed with a numerical validation of both the standard and the entropic realizations of the consistent two-population lattice Boltzmann equation in Sec. III.

### G. Comparison to other two-population thermal models based on the energy conservation

While we have already discussed the difference of the present approach from [20], in this section we shall explain the difference from the thermal model of Ref. [22]. As it was already mentioned in the Introduction, the model of Ref. [22] is also based on the total energy rather than on the thermal energy. In the present notation, the model [22] can be written [for the purpose of a comparison, it is sufficient to consider the

space-time continuous version, and we have taken into account the factor two in the definition of the energy (3)]:

$$\partial_t f_i + \boldsymbol{v}_i \cdot \nabla f_i = -\omega\big(f_i - f_i^{\mathrm{eq}}\big), \tag{101}$$

$$\partial_t g_i + \boldsymbol{v}_i \cdot \nabla g_i = -\omega_1\big(g_i - g_i^{\mathrm{eq}}\big) + (\omega_1 - \omega)(2\boldsymbol{v}_i \cdot \boldsymbol{u} - u^2) \times \big(f_i - f_i^{\mathrm{eq}}\big), \tag{102}$$

whereas the present kinetic equation reads

$$\partial_t f_i + \boldsymbol{v}_i \cdot \nabla f_i = -\omega\big(f_i - f_i^{\mathrm{eq}}\big), \tag{103}$$

$$\partial_t g_i + \boldsymbol{v}_i \cdot \nabla g_i = -\omega\big(g_i - g_i^{\mathrm{eq}}\big) + (\omega - \omega_1)(g_i - g_i^{*}). \tag{104}$$

Both the present model and the model of Ref. [22] use the same equilibria $f^{\mathrm{eq}}$ (84) and $g^{\mathrm{eq}}$ (85). However, they are different because, as we shall see it below, they result in different moment systems.

In order to make explicit the difference between the two models, let us write down the relaxation equations for the moments of $g$ populations. Both (102) and (104) give the same relaxation equations for the energy and the energy flux:

$$\partial_t^{\mathrm{relax}}(2\rho E) = 0, \tag{105}$$

$$\partial_t^{\mathrm{relax}} q_\alpha = -\omega_1\big(q_\alpha - q_\alpha^{\mathrm{eq}}\big) + 2(\omega_1 - \omega)u_\beta\big(P_{\alpha\beta} - P_{\alpha\beta}^{\mathrm{eq}}\big). \tag{106}$$

However, the relaxation of the *flux of energy flux*, $R_{\alpha\beta} = \sum_{i=0}^{Q} v_{i\alpha} v_{i\beta} g_i$, is different for both models:

$$\partial_t^{\mathrm{relax}} R_{\alpha\beta} = -\omega_1\big(R_{\alpha\beta} - R_{\alpha\beta}^{\mathrm{eq}}\big), \quad \text{(present)} \tag{107}$$

$$\partial_t^{\mathrm{relax}} R_{\alpha\beta} = -\omega_1\big(R_{\alpha\beta} - R_{\alpha\beta}^{\mathrm{eq}}\big) + (\omega_1 - \omega)\big[2u_\gamma\big(Q_{\gamma\alpha\beta} - Q_{\gamma\alpha\beta}^{\mathrm{eq}}\big) - u^2\big(P_{\alpha\beta} - P_{\alpha\beta}^{\mathrm{eq}}\big)\big], \quad \text{(Ref.[22])}, \tag{108}$$

where $Q_{\alpha\beta\gamma} = \sum_{i=0}^{Q} v_{i\alpha} v_{i\beta} v_{i\gamma} f_i$, and $Q_{\alpha\beta\gamma}^{\mathrm{eq}}$ is given by Eq. (20). While both the present model and that of Ref. [22] lead to same equations in the hydrodynamic limit, they are different in nature. In the present approach, the local coupling is maintained through the *pertinent moments* of the $f$ populations only [the nonequilibrium stress tensor in the quasiequilibrium population $g^*$ (86)], while in the model of Ref. [22] it is achieved through the nonequilibrium part of the $f$ population itself. For that reason, in particular, it is unclear whether the model of Ref. [22] can be extended to the entropic formulation. Indeed, the subgrid features of the entropic realization of Sec. II F are expected to maintain "good" properties of stresses only, while the behavior of the individual populations need not be smooth.

The above analysis explains the difference between the two approaches to the construction of two-population lattice Boltzmann models. Yet another interpretation can be offered as follows: The model of Ref. [22], Eq. (102), can be rewritten as

$$\partial_t g_i + \boldsymbol{v}_i \cdot \nabla g_i = -\omega\big(g_i - g_i^{\mathrm{eq}}\big) + (\omega - \omega_1)(g_i - G_i), \tag{109}$$

where

$$G_i = g_i^{\mathrm{eq}} + Z_i\big(f_i - f_i^{\mathrm{eq}}\big), \tag{110}$$

with $Z_i = (2\boldsymbol{v}_i \cdot \boldsymbol{u} - u^2)$. On the other hand, the quasiequilibrium of the present model, Eq. (86), can be represented as

$$g_i^{*} = g_i^{\mathrm{eq}} + W_i \frac{2v_{i\alpha}u_\beta\big(P_{\alpha\beta} - P_{\alpha\beta}^{\mathrm{eq}}\big)}{T_0}. \tag{111}$$

Thus, the two models are different by the second term in $G_i$ (110) and that in the present quasiequilibrium $g_i^*$ (111). In Ref. [22], the function $Z_i(f_i - f_i^{\mathrm{eq}})$ was obtained upon a direct discretization of the term $R(\boldsymbol{v}) = Z(\boldsymbol{v})(f(\boldsymbol{v}) - f^{\mathrm{eq}}(\boldsymbol{v}))$, where $Z(\boldsymbol{v}) = 2\boldsymbol{v} \cdot \boldsymbol{u} - u^2$ and $f^{\mathrm{eq}}(\boldsymbol{v})$ is the Maxwell-Boltzmann distribution function, in a continuous-velocity kinetic model proposed therein. However, a consistent evaluation of the term $R(\boldsymbol{v})$ in their continuous-velocity kinetic equation using the Hermite polynomial expansion (see Ref. [17] for details) would instead produce the term,

$$R(\boldsymbol{v}) \approx W(\boldsymbol{v}) \frac{2v_\alpha u_\beta\big(P_{\alpha\beta} - P_{\alpha\beta}^{\mathrm{eq}}\big)}{T}, \tag{112}$$

where $W(\boldsymbol{v}) = (2\pi T)^{-D/2} \exp\big(-|\boldsymbol{v}|^2/2T\big)$, and which leads to the present expression (111) rather than to (110) upon the discretization of the continuous-velocity space. Finally, we mention that the model of Ref. [22] was recently extended to a compressible flow case in Ref. [27], along the lines of Ref. [19]. Obviously, the present model can be also extended to a compressible case along the same lines.

Since both the present model and the model of Ref. [22] recover the same hydrodynamic equations, there is no significant difference between the two in a fully resolved direct numerical simulation. However, the present model allows for the entropic formulation which amounts to a built-in subgrid model (cf. Sec. II F and [9,10]). In the next section, we shall validate the entropic formulation of the present model numerically.

## III. NUMERICAL VALIDATION

In order to validate the new thermal lattice Boltzmann model, simulations of a planar Couette flow with walls at different temperatures and of the Rayleigh-Bénard convection problem were conducted. The choice of the benchmarks is the same as in [20]. All simulations were executed in two dimensions with the $D2Q9$ lattice.

### A. Couette flow

In order to validate that the viscous heating is recovered by the proposed model, the Couette flow with a temperature gradient was simulated. The bottom wall of the slab was stationary and was kept at a constant temperature $T_C$. The top wall was moved at a constant speed $U$ and was kept at a temperature $T_H$, where $T_H > T_C$. Analytical solution for the

temperature profile in this case is as follows:

$$\frac{T - T_C}{T_H - T_C} = \frac{y}{H} + \frac{\mathrm{Pr} \times \mathrm{Ec}}{2} \frac{y}{H} \left(1 - \frac{y}{H}\right), \qquad (113)$$

where $y$ is the distance from the bottom wall; $H$ is the height of the channel; $\mathrm{Pr} = \mu/\kappa$ is the Prandtl number; $\mathrm{Ec} = U^2/(c_v(T_H - T_C))$ is the Eckert number, $c_v = 1$. Simulations were performed in a wide range of Prandtl numbers and Eckert numbers. If not mentioned otherwise, in all simulations the following parameters were used: $U = 0.05$, $H = 100$, $T_C = 1.0$, $\mu = 0.025$. All other parameters are defined from the Prandtl and Eckert numbers. The periodic boundary condition was applied in the $x$ direction. On the top and bottom walls, the recently introduced Tamm–Mott-Smith (TMS) boundary conditions [10] were used.

For the sake of completeness, the boundary condition for the top wall is presented (see Fig. 1); the implementation at the bottom wall is similar. As the proposed model splits the conservation laws between the two populations the boundary condition has to be applied on both populations. We therefore used the same boundary condition for the $f$ and $g$ populations. If not otherwise mentioned the description holds for the $f$ and $g$ populations even if only the formulas for the $f$ populations are provided.

In the first step the boundary condition has to approximate the missing distributions. This is done by assigning equilibrium values computed at $\rho_{\mathrm{tgt}}$ and $U_{\mathrm{wall}}$. Where $\rho_{\mathrm{tgt}}$ is computed from the no-flux condition or equivalently in this case from the bounce-back condition,

$$f_7 = f_5, \quad f_4 = f_2, \quad f_8 = f_6. \qquad (114)$$

As now all distributions are known the current equilibrium distributions $f_i^{\mathrm{eq}}$ and $g_i^{\mathrm{eq}}$ are calculated. In addition to the local equilibrium the equilibrium at given target values is calculated $f_i^{\mathrm{eq}}(\rho_{\mathrm{tgt}}, U_{\mathrm{wall}})$ and $g_i^{eq}(T_{\mathrm{wall}}, U_{\mathrm{wall}}, \rho_{\mathrm{tgt}})$. The target values are the density $\rho_{\mathrm{tgt}}$; the velocity $U_{\mathrm{wall}}$ and temperature $T_{\mathrm{wall}}$ we want to enforce at the wall. Thus, the pre-collision values of

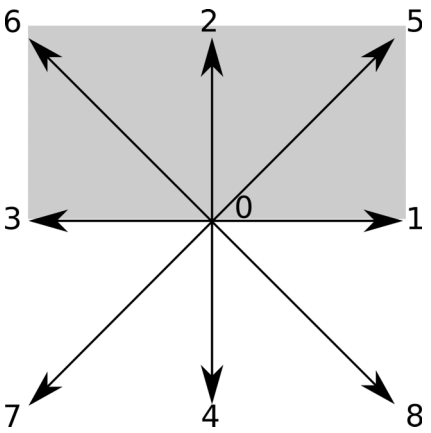


FIG. 1. Sketch of the discrete velocities at the top wall. Populations 7, 4, and 8 are missing after the propagation step and are completed by the bounce-back rule (114).

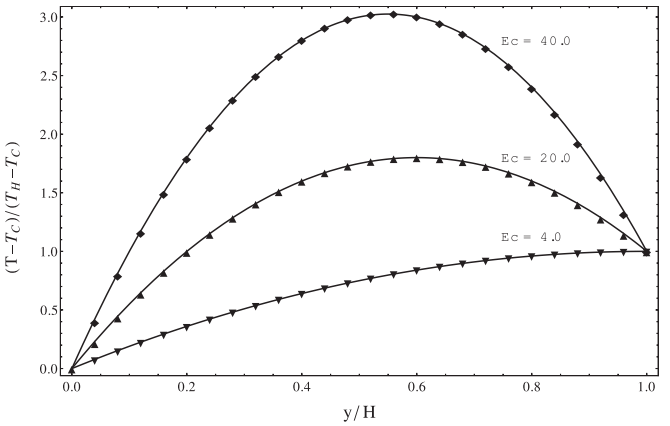


FIG. 2. Temperature profile of the Couette flow at various Eckert numbers, where the Prandtl number is fixed to $\mathrm{Pr} = 0.5$. The solid line represents the analytical solution; the symbols are the simulation results.

the populations on the boundary nodes are [10]

$$f_i \to f_i + f_i^{\mathrm{eq}}(\rho_{\mathrm{tgt}}, U_{\mathrm{wall}}) - f_i^{\mathrm{eq}}, \qquad (115)$$

$$g_i \to g_i + g_i^{\mathrm{eq}}(T_{\mathrm{wall}}, U_{\mathrm{wall}}, \rho_{\mathrm{tgt}}) - g_i^{\mathrm{eq}}, \quad \forall i = 0, \ldots, Q. \qquad (116)$$

The collision step is then applied on the boundary nodes for both $f$ and $g$ populations in the usual way.

In the present simulation, results are practically identical for both the standard and the entropic lattice Boltzmann formulations; hence only the results obtained by the standard lattice Boltzmann are presented here. In Fig. 2 the results for $\mathrm{Pr} = 0.5$ and $\mathrm{Ec} = 4$, 20, and 40 are shown; Fig. 3 demonstrates the results for $\mathrm{Ec} = 8.0$ and $\mathrm{Pr} = 0.25$, 1.25, and 2.5. Figures 2 and 3 demonstrate that simulation recovers the analytical solution with good accuracy.

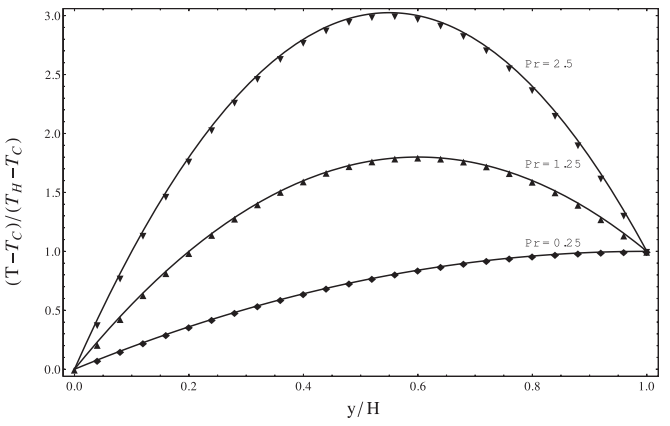


FIG. 3. Temperature profile of the Couette flow at various Prandtl numbers, where the Eckert number is fixed to $\mathrm{Ec} = 8.0$. The solid line represents the analytical solution; the symbols are the simulation results.

### B. Rayleigh-Bénard convection

For a further validation of the proposed model, the Rayleigh-Bénard convection was analyzed. In the Rayleigh-Bénard convection a horizontal layer of viscous fluid is heated by the bottom wall with temperature $T_H$ and cooled by the top wall at temperature $T_C$. For small Rayleigh numbers [defined as $\mathrm{Ra} = G\lambda(T_H - T_C)H^3/(\mu\kappa)$, where $G$ is acceleration due to gravity] a static solution exists, where a constant temperature gradient is developed between the hot and cold wall. If the Rayleigh number is increased above a certain threshold the static temperature gradient becomes unstable and the system starts to convect. For this simulation, a buoyancy force needs to be applied on the $f$ populations.

The force was implemented in the present scheme following the method of Kupershtokh (so-called exact difference method, [28]; see, however, Ref. [29] for a discussion and possible alternatives); that is, the kinetic Eqs. (97) and (98) are modified as follows with respect to the $f$ populations:

$$f_i(\boldsymbol{x}+\boldsymbol{v}_i,t+1) - f_i(\boldsymbol{x},t) = \alpha\beta\left(f_i^{\mathrm{eq}}(\rho,\boldsymbol{u}) - f_i\right) + \left[f_i^{\mathrm{eq}}(\rho,\boldsymbol{u}+\Delta\boldsymbol{u}) - f_i^{\mathrm{eq}}(\rho,\boldsymbol{u})\right], \tag{117}$$

$$g_i(\boldsymbol{x}+\boldsymbol{v}_i,t+1) - g_i(\boldsymbol{x},t) = \omega_1(g_i^* - g_i) + 2\beta\left(g_i^{\mathrm{eq}} - g_i^*\right), \tag{118}$$

where the added term on the right-hand side of (117) takes into account the change of the velocity due to the presence of the acceleration $\boldsymbol{a}$ per time step $\delta t = 1$: $\Delta\boldsymbol{u} = \boldsymbol{a}\delta t$. In the Boussinesq approximation,the buoyancy force can be written as

$$\rho\boldsymbol{a} = \rho\lambda G(T - T_{\mathrm{m}})\boldsymbol{i}, \tag{119}$$

where $\lambda$ is the thermal expansion coefficient; $G$ is the acceleration due to the gravity; $T_{\mathrm{m}} = (T_C + T_H)/2$ is the mean temperature of the cold and hot wall; $\boldsymbol{i}$ is a unit vector pointing from the hot to the cold wall. The boundary conditions were the same as for the Couette flow benchmark.

The Rayleigh-Bénard convection simulations were initialized with the linear temperature field,

$$T(x,y) = T_H - \Delta T\frac{y}{H}, \tag{120}$$

where $\Delta T = T_H - T_C$ is the temperature difference between the cold and hot wall; $y$ is the distance from the bottom wall; $H$ is the distance between the walls. Following [20], the initial density was subject to a perturbation,

$$\rho = \left[1 + \frac{\rho\lambda G\Delta T y}{2}\left(1 - \frac{y}{H}\right)\right]\left[1 + 0.001\cos\left(\frac{2\pi x}{L}\right)\right], \tag{121}$$

where $L$ is the length of the channel.

Snapshots of the temperature distributions of the Rayleigh-Bénard convection after $3 \times 10^4$ time steps are

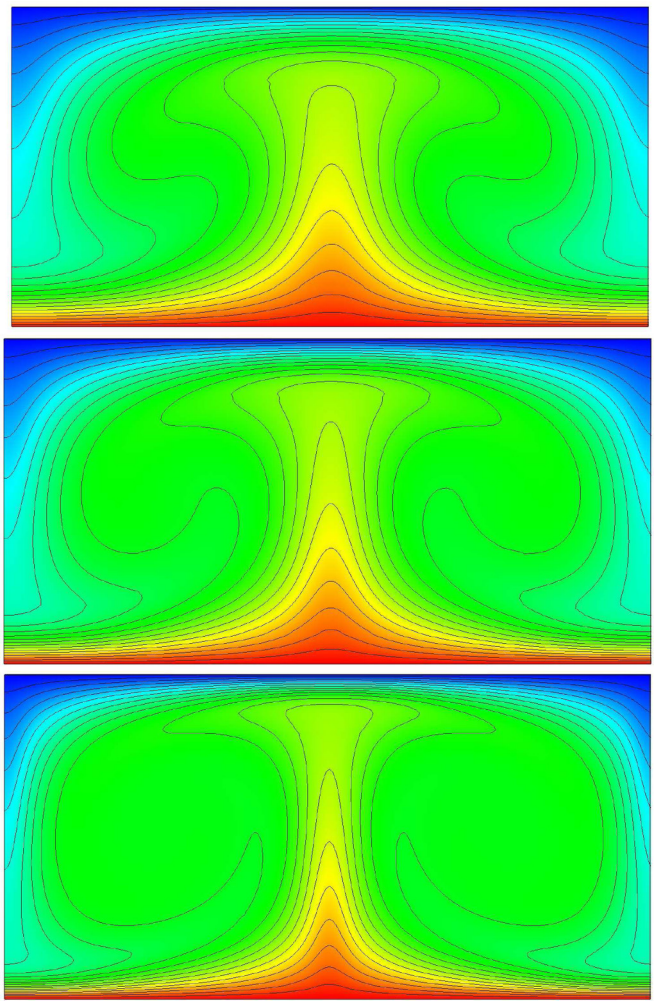

FIG. 4. (Color online) Snapshots of the reduced temperature in the range [0,1] (blue to red), at various Rayleigh number after $3 \times 10^4$ time steps. (Top) $\mathrm{Ra} = 2 \times 10^4$; (center) $\mathrm{Ra} = 5 \times 10^4$; (bottom) $\mathrm{Ra} = 2 \times 10^5$. A total of 10 uniformly spaced temperature contours with an interval of 0.1 are displayed. Temperature is in lattice units.

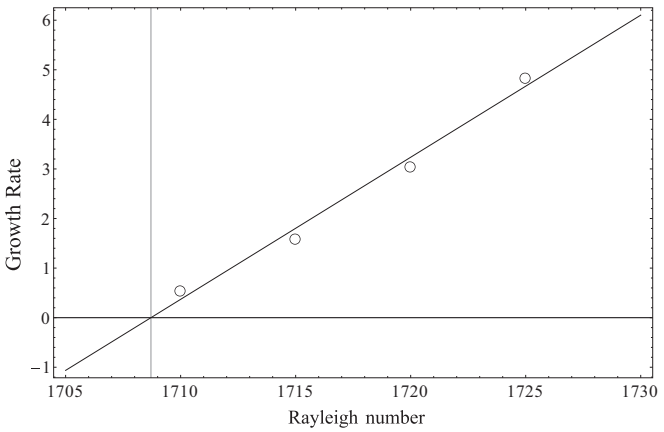


FIG. 5. Growth rate ($\times 10^3$) of the velocity are found to depend linearly on the Rayleigh number near $\mathrm{Ra_c}$. Circles are the measurements; the diagonal line is the linear fit to the measurements. The critical Rayleigh number, $\mathrm{Ra_c} = 1708.71$, is obtained by extrapolation of the data to the zero growth rate.

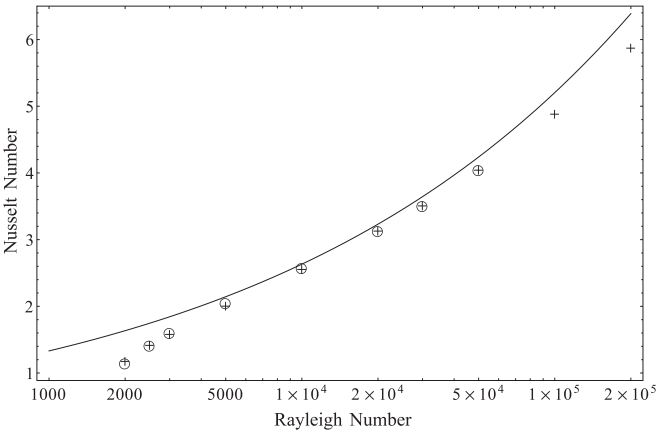


FIG. 6. Dependence of the Nusselt number on the Rayleigh number. (Line) Empirical formula, $\mathrm{Nu} = 1.56(\mathrm{Ra}/\mathrm{Ra_c})^{0.296}$ [20]; (circle) reference values [30]; (cross) present ELBM simulation.

presented in Fig. 4 for $\mathrm{Ra} = 2 \times 10^4$, $\mathrm{Ra} = 5 \times 10^4$, and $\mathrm{Ra} = 2 \times 10^5$, respectively.

As seen from the figures the expected trends are recovered: The higher the Rayleigh number the better the cold and hot fluid are mixed and the temperature gradient is increased near the top and bottom walls.

As a first test, the critical Rayleigh number in a fully resolved simulation ($400 \times 200$ grid points) was analyzed. For that, the growth rate $r$ of the velocity in the middle of the domain was measured,

$$r = \frac{v_m(t) - v_m(t-1)}{v_m(t-1)}, \tag{122}$$

where $v_m(t) = \sum_{k=0}^{H} [u(L/2,k,t)]^2$. The growth rate was analyzed at Rayleigh numbers slightly above the critical Rayleigh number. The critical Rayleigh number was obtained by extrapolation of the measurements to the zero growth rate (see Fig. 5). The critical Rayleigh number from the present simulation is $\mathrm{Ra_c} = 1708.71$, and is in good agreement with the theoretical value $\mathrm{Ra_c} = 1707.76$ [20].

Above the critical Rayleigh number the heat transfer between the cold and hot walls is increased, and the Rayleigh-Bénard convection is established. The Nusselt number Nu describes the increased heat transfer:

$$\mathrm{Nu} = \frac{H}{\kappa \Delta T} \left\{ \frac{1}{L} \sum_{k=1}^{k=L} \left[ u_y T - \kappa \frac{\partial T(k,y)}{\partial y} \right] \right\}, \tag{123}$$

where $L$ is the size of the lattice in the $x$ direction, and the derivative was realized as the second-order finite difference. For the results presented the mean value of the Nusselt number at the hot and cold walls was used. In Fig. 6 one can see that the reference results [30] are recovered with excellent accuracy using a $200 \times 100$ grid. With the two-population ELBM, stable simulations could be performed to at least $\mathrm{Ra} = 10^9$ on a $100 \times 51$ grid. However, for Rayleigh numbers above $\sim 10^5$ both the ELBM and the conventional realization without the entropy estimate start to underestimate the heat transfer. This trend was also observed by others [20,31], and indicates limitations of the two-dimensional model. A further detailed study of natural convection using the three-dimensional ELBM is beyond the scope of this paper, and will be reported elsewhere.

## IV. CONCLUSION

We have revisited the two-population approach to deriving lattice Boltzmann models for the simulation of thermal flows introduced in [20]. We have demonstrated in detail that the approach of [20] becomes greatly enhanced both in terms of simplicity of the model, its robustness, and physical relevance only if the physical conservation law of energy is used and not the artificial conservation of the thermal energy. The resulting model was realized for the much studied standard lattices, and shares the same degree of simplicity as the conventional LB model for isothermal flow. The model is free of assumptions other than the standard low Mach number limitation of the conventional LB method. The newly proposed model was also extended to the entropic LB scheme for subgrid simulations. The numerical validation with the commonly used benchmark problems in two dimensions shows excellent performance and accuracy of the present model. We believe that the present model provides a very natural extension of the standard isothermal LB method, and can be useful in simulating low Mach number engineering flow problems with temperature variation.

## ACKNOWLEDGMENTS

This work was supported by the European Research Council (ERC) Advanced Grant No. 291094-ELBM; a part of the computational resources was provided by Swiss National Supercomputing Center-CSCS under Grant No. s437.

[1] H. Chen, S. Kandasamy, S. Orszag, R. Shock, S. Succi, and V. Yakhot, Science **301**, 633 (2003).
[2] S. Succi, *The Lattice Boltzmann Equation for Fluid Dynamics and Beyond* (Oxford University Press, Oxford, 2001).
[3] M. Mendoza, I. Karlin, S. Succi, and H. J. Herrmann, Phys. Rev. D **87**, 065027 (2013).
[4] S. Succi, R. Benzi, and M. Vergassola, Phys. Rep. **222**, 145 (1992).
[5] H. Chen, S. Chen, and W. H. Matthaeus, Phys. Rev. A **45**, R5339 (1992).
[6] Y. H. Qian, D. d'Humieres, and P. Lallemand, Europhys. Lett. **17**, 479 (1992).
[7] S. Chen and G. D. Doolen, Annu. Rev. Fluid Mech. **30**, 329 (1998).
[8] I. V. Karlin, A. Ferrante, and H. C. Öttinger, Europhys. Lett. **47**, 182 (1999).

[9] I. V. Karlin, S. Succi, and S. S. Chikatamarla, Phys. Rev. E **84**, 068701 (2011).
[10] S. Chikatamarla and I. Karlin, Physica A **392**, 1925 (2013).
[11] F. J. Alexander, S. Chen, and J. D. Sterling, Phys. Rev. E **47**, R2249 (1993).
[12] G. R. McNamara, A. L. Garcia, and B. J. Alder, J. Stat. Phys. **81**, 395 (1995).
[13] S. S. Chikatamarla and I. V. Karlin, Phys. Rev. Lett. **97**, 190601 (2006).
[14] S. S. Chikatamarla and I. V. Karlin, Phys. Rev. E **79**, 046701 (2009).
[15] S. S. Chikatamarla, C. E. Frouzakis, I. V. Karlin, A. G. Tomboulides, and K. B. Boulouchos, J. Fluid Mech. **656**, 298 (2010).
[16] D. N. Siebert, L. A. Hegele, and P. C. Philippi, Phys. Rev. E **77**, 026707 (2008).
[17] X. W. Shan, X. Yuan, and H. Chen, J. Fluid Mech. **550**, 413 (2006).
[18] Y. H. Qian and S. A. Orszag, Europhys. Lett. **21**, 255 (1993).
[19] N. I. Prasianakis and I. V. Karlin, Phys. Rev. E **76**, 016702 (2007).
[20] X. He, S. Chen, and G. D. Doolen, J. Comput. Phys. **146**, 282 (1998).
[21] Y. Peng, C. Shu, and Y. T. Chew, Phys. Rev. E **68**, 026701 (2003).
[22] Z. Guo, C. Zheng, B. Shi, and T. S. Zhao, Phys. Rev. E **75**, 036704 (2007).
[23] S. Ansumali, S. Arcidiacono, S. S. Chikatamarla, N. I. Prasianakis, A. N. Gorban, and I. V. Karlin, Eur. Phys. J. B. **56**, 135 (2007).
[24] C. D. Levermore, J. Stat. Phys. **83**, 1021 (1996).
[25] A. N. Gorban and I. V. Karlin, Physica A **206**, 401 (1994).
[26] S. S. Chikatamarla, S. Ansumali, and I. V. Karlin, Europhys. Lett. **74**, 215 (2006).
[27] Q. Li, K. H. Luo, Y. L. He, Y. J. Gao, and W. Q. Tao, Phys. Rev. E **85**, 016710 (2012).
[28] A. L. Kupershtokh, in *Proceedings for 5th International EDH Workshop* (University of Poitiers, Poitiers, France, 2004), pp. 241–246.
[29] Q. Li, K. H. Luo, and X. J. Li, Phys. Rev. E **86**, 016709 (2012).
[30] R. M. Clever and F. H. Busse, J. Fluid Mech. **65**, 625 (1974).
[31] X. W. Shan, Phys. Rev. E **55**, 2780 (1997).